Radiation Damage in Silicon Detectors[†]

Gunnar Lindström[*]

Institute for Experimental Physics, University of Hamburg, 22761 Hamburg, Germany

Abstract

Radiation damage effects in silicon detectors under severe hadron- and γ–irradiation are surveyed, focusing on bulk effects. Both macroscopic detector properties (reverse current, depletion voltage and charge collection) as also the underlying microscopic defect generation are covered. Basic results are taken from the work done in the CERN-RD48 (ROSE) collaboration updated by results of recent work. Preliminary studies on the use of dimerized float zone and Czochralski silicon as detector material show possible benefits. An essential progress in the understanding of the radiation induced detector deterioration had recently been achieved in gamma irradiation, directly correlating defect analysis data with the macroscopic detector performance.

Keywords: silicon detectors; defect emgineering; radiation damage; NIEL; proton-, neutron-, π-irradiation; defect analysis

---

[†] Invited talk presented at the 9th European Symposium on Semiconductor Detectors, Schloss Elmau, Germany, June 23-27, 2002; accepted for publication in Nucl. Instr. and Meth. A

[*] Corresponding author. Tel.: +49-40-8998-2951; fax: +49-40-8998-2959; e-mail: gunnar.lindstroem@desy.de

1. Introduction

Silicon pixel and microstrip detectors are today's best choices for meeting the requirements of tracking applications in the forthcoming LHC experiments. However, due to the extreme harsh radiation environment the required prolonged operability poses an unprecedented challenge to their radiation tolerance. At the expected yearly level of up to several 10^{14} hadrons per cm² during the foreseen 10 years of operation the damage induced changes in the silicon bulk will cause an increase of both the reverse current and the necessary depletion voltage as well as a decrease of the charge collection efficiency. Using standard silicon material and present detector technology these damage induced effects lead to not tolerable deteriorations in the detector performance. Possible strategies for improving the radiation hardness of these devices consist of using suitable defect engineering of the silicon material, as introduced by the CERN-RD48 (ROSE) collaboration [1], operation at very low temperatures under investigation by the CERN-RD39 group [2] or a specialized design of detector geometry, presently proposed or under test by several other groups, see e.g. [3] and literature cited there.

This report is based on the results of the ROSE collaboration showing the appreciable improvements which had been achieved by diffusing oxygen from the SiO_2-Si interface into the silicon bulk after initial oxidation of the silicon wafers. This so called DOFZ (Diffusion Oxygenated Float Zone) technology had proven to be the most cost effective way of adequately modifying the standard process technology (see section 4.1).

In the following different aspects of hadron and gamma/lepton induced bulk damage effects, originating from the Non Ionizing Energy Loss (NIEL) are summarized, especially comparing standard with oxygenated silicon detectors, as extracted from numerous publications of the ROSE collaboration [4]. In contrast to bulk effects surface and interface related changes, produced by the ionizing energy loss (radiation dose), play a minor role for lifetime limitations of silicon detectors. The discussion of such effects can e.g. be found in [5].

2. Primary damage effects

The bulk damage in silicon detectors caused by hadrons or higher energetic leptons respectively gammas is primarily due to displacing a Primary Knock on Atom PKA out of its lattice site. The threshold energy for this process is ~ 25 eV. Such single displacements resulting in a pair of a silicon interstitial and a vacancy (Frenkel pair) can be generated by e.g. neutrons or electrons with an energy above 175 eV and 260 keV respectively. Low energy recoils above these threshold energies will usually create fixed point defects. However for recoil energies above about 5 keV a dense agglomeration of defects is formed at the end of the primary PKA track. Such disordered regions are referred to as defect clusters. The kinematic lower limits for the production of clusters are ~35 keV for neutrons and ~8 MeV for electrons. In figure 1 the simulation result for a 50 keV PKA (average recoil produced by 1 MeV neutrons) is shown, clearly distinguishing between discretely distributed vacancies (point defects) and dense agglomerates (clusters) [6]. It should be noted here that the radiation damage caused by Co-60 gammas is primarily due to the interaction of Compton electrons having a maximum energy of only 1 MeV. Hence in this case cluster production is not possible and the damage is exclusively due to point defects.

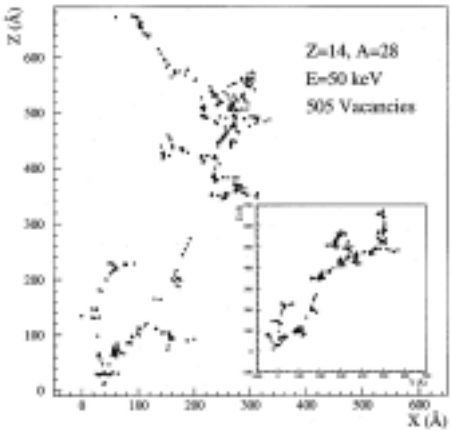

Fig. 1. Simulation results: Sample distribution of vacancies induced by a 50 keV recoil silicon atom; insert shows transverse projection [6].

Both point defects and clusters can have severe effects on the detector performance, depending on their concentration, energy level and the respective electron and hole capture cross section. Defects with deep energy levels in the middle of the forbidden gap could act as recombination/generation centers and are hence responsible for an increase of the reverse detector current. The removal of dopants by formation of complex defects as well as the generation of charged centers changes the effective doping concentration and the needed operating voltage to fully deplete the detector thickness. Finally such defects could also act as trapping centers affecting the charge collection efficiency. In view of the LHC operational scenario it has also to be noted that the primary produced defects may be subject to changes after long term storage at room temperature. Such annealing effects may very likely be caused by changes due to the dissolution of clusters releasing migrating vacancies and interstitials [7]. The observed time constants for such "reverse annealing" processes are rather large (for standard silicon at room temperature e.g. ~ 1year). A reliable projection of damage results on the LHC operational scenario is hence only possible if annealing effects are included comparable to those expected in 10 years of LHC operation. This task had been successfully attacked by performing studies at elevated temperatures thus accelerating the kinetic effects being responsible for such long term changes. Related basic studies are found in [8-10].

3. NIEL scaling of bulk damage

The preceding discussion and numerous experimental observations have led to the assumption that damage effects produced in the silicon bulk by energetic particles can be described as being proportional to the so called displacement damage cross section D. This quantity is equivalent to the Non Ionizing Energy Loss (NIEL) and hence the proportionality between the NIEL-value and the resulting damage effects is referred to as the NIEL-scaling hypothesis (for deviations to this rule see section 4.5.1). The displacement damage cross section D is normally quantified in MeVmb, whereas the NIEL-value is given in keVcm²/g. For silicon with A=28.086 g/mol the relation between D and NIEL is:

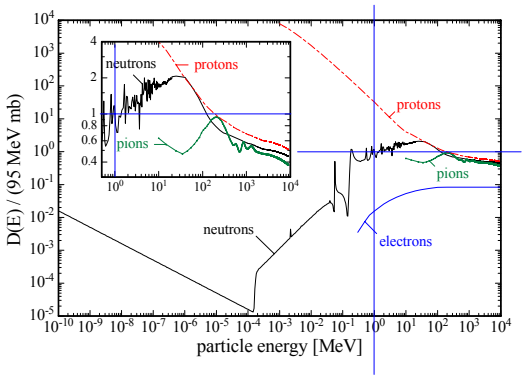

Fig. 2. Non ionising energy loss NIEL for different particles.

100 MeVmb = 2.144 keVcm²/g. The D or NIEL value is depending on the particle type and energy. According to an ASTM standard, the displacement damage cross section for 1 MeV neutrons is set as a normalizing value: $D_n(1MeV) = 95$ MeVmb [11]. On the basis of the NIEL scaling the damage efficiency of any particle with a given kinetic energy can then be described by the hardness factor κ. Applying the NIEL hypothesis, one may replace the actual particle energy spectrum $d\Phi/dE$ by a NIEL folded spectrum and the damage effect, caused by its total fluence Φ_p by a 1MeV neutron equivalent fluence $\Phi_{eq} = \kappa \cdot \Phi_p$, a more detailed discussion is found in [12, 13].

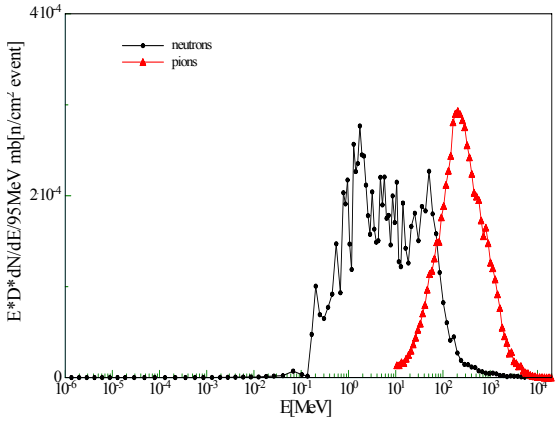

Fig. 3. NIEL folded energy spectra for neutrons and pions in the SCT region (silicon counter tracker) of the LHC ATLAS detector.

In figure 2 the normalized NIEL values are plotted as function of energy. The data are taken from [14-17]. More recent calculations can be found in [6], [18]. NIEL scaling and its limitations is extensively discussed in [6]. Regardless of possible deviations in certain cases, the NIEL scaling should always be applied as a first order approximation of the damage efficiency. Hence it is useful to display the NIEL folded energy spectra for the most abundant particles (neutrons and pions) in the LHC experiments, as done for the SCT region of ATLAS in figure 3 [12]. Finally the resulting equivalent fluences as function of radius are shown in figure 4.

From figure 3 we conclude that reactor neutrons, ranging mainly from 1 to 10 MeV, are adequate for reliable damage tests and that indeed irradiations with 250 MeV pions, available at PSI-Villigen, should result in similar damage as expected in LHC. Many of the past and present irradiation tests have however been performed using the 23 GeV proton beam at CERN-PS. In view of reliable predictions for the LHC performance it is therefore reassuring that damage results from 23 GeV proton and 250 MeV pion irradiation agree pretty well, if proper NIEL scaling is used.

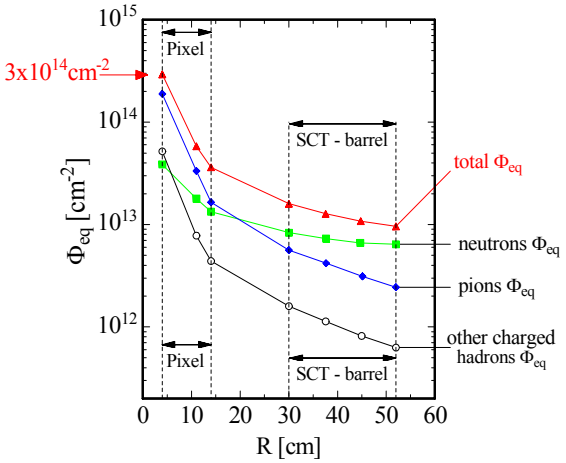

Fig. 4. Hadron fluences expected in the ATLAS inner detector.

4. Survey of damage results

4.1. DOFZ technology

The key idea of the RD48 strategy implied that the radiation tolerance of silicon can be improved by adequate defect engineering. Defect engineering involves the deliberate addition of impurities in order to reduce the damage induced formation of electrically active defects. Based on early attempts at the Instrumentation Division of BNL [19], RD48 relied on carbon and oxygen as the key ingredients for reaching this goal [1]. A wide range of oxygen and carbon concentrations had been investigated using several different process technologies.

It was finally found that an oxygen enrichment can best be achieved by a post-oxidation diffusion of oxygen into the silicon bulk. This DOFZ process (Diffusion Oxygenated Float Zone) has been performed at temperatures between 1100 and 1200°C and with durations between several hours and 10 days, reaching an oxygen concentration between 1 and $4 \cdot 10^{17}$ O/cm³ (see also figure 23).

Practical applications are employing a diffusion at 1150°C for 24-72h. The O-concentration reached this way is around $2 \cdot 10^{17}$ O/cm³, see figure 5.

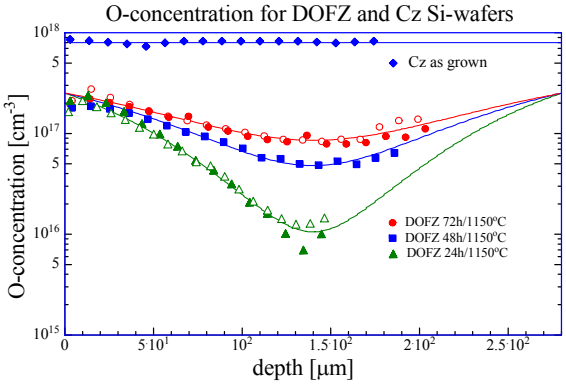

Fig. 5. Depth profiles of O-concentration for three different DOFZ processes, from bottom: 24, 48, 72 h at 1150 ºC; in comparison: Czochralski silicon; measured by SIMS [20, 21].

It should be emphasized that the DOFZ process can easily be included in the standard detector process

technology and had proven to be a most cost effective technique. It was meanwhile successfully transferred to several manufacturing companies, see [22] and is e.g. employed in the design and processing of pixel and microstrip detectors for the ATLAS experiment [23].

4.2. bulk generation current

The damage induced increase of the bulk generation current ΔI exhibits a quite simple dependence on the irradiating particle type and fluence.

If normalized to the sensitive volume V (best defined by using a guard ring structure around the diode pad), the current increase is strictly proportional to the 1 MeV neutron equivalent fluence Φ_{eq} (see section 3), as demonstrated in figure 6 [10]. Therefore a "current related damage rate α" can be defined by:

$$\Delta I/V = \alpha \cdot \Phi_{eq} \qquad (1)$$

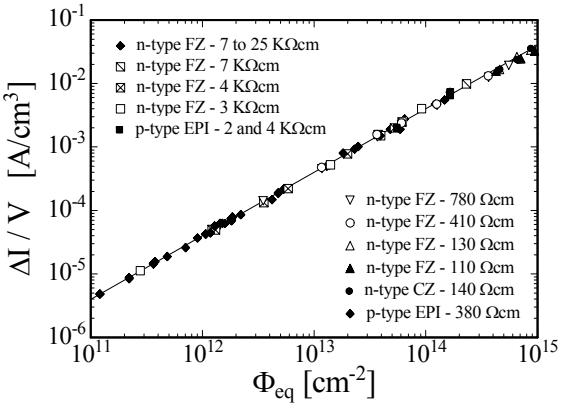

Fig. 6. Damage induced bulk current as function of particle fluence for different detector types.

The measured value of the reverse current depends exponentially on the operating temperature in a straight forward way and α-values are therefore always normalized to 20°C. Details for this normalization and the temperature dependent beneficial annealing, depicted in figure 7, can be found in [10, 24]. At any given temperature and

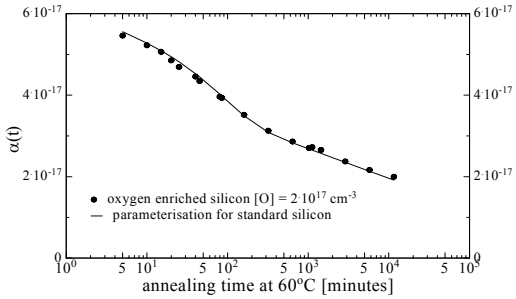

Fig. 7. Annealing function of current related damage parameter α for standard (solid line) and DOFZ (dots) silicon detectors.

annealing time the damage rate α, if temperature normalized, is a universal constant, not depending on the material type (n- or p-type, FZ, epi or Cz silicon, resistivity), or irradiating particles (neutrons, protons, pions). Therefore α is often used to reliably monitor the accumulated particle fluence. A recommendation for this task is its measurement after an annealing of 80 min at 60°C. In this situation α is independent of the detailed history of the actual irradiation. The ROSE adapted value is: $\alpha_{80/60} = 4.0 \cdot 10^{-17}$ A/cm. For an annealing temperature of 80°C the same value would be reached after an annealing time of ~10 minutes [10, 25].

It should be emphasized that the bulk current increase and its annealing function follow strictly the NIEL scaling. This and the observation, that the large current values cannot be explained by any known discrete point defects led to the assumption of a cluster related effect. The correlation with the enhanced density of double vacancies in clusters as observed in [25] and a possible interstate charge transfer mechanism, as proposed in [26], are likely explanations.

4.3. effective doping and depletion voltage

The depletion voltage V_{dep}, necessary to fully extend the electric field throughout the depth d of the detector (asymmetric junction) is related with the effective doping concentration N_{eff} of the silicon bulk

by

$$V_{dep} = (q_0/2\varepsilon\varepsilon_0)|N_{eff}|d^2 \qquad (2)$$

This equation holds not only for the original n-type silicon (donor doped) but also after severe irradiation when the effective doping concentration changes its sign by increased generation of "acceptor like" defects. In any case one can describe the change of the depletion voltage by the related change in $|N_{eff}| = |N_d - N_a|$ with N_d and N_a as the positively charged donor and negatively charged acceptor concentration.

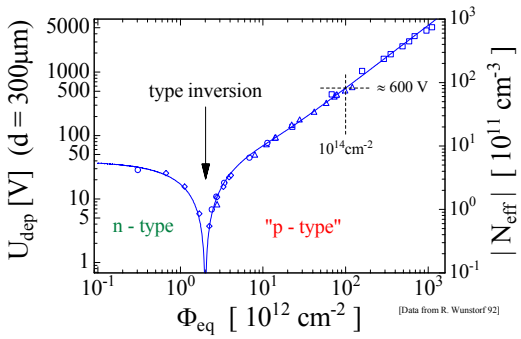

Fig. 8. Change of the effective doping concentration in standard silicon, as measured immediately after neutron irradiation.

The result of a first systematic study of the extremely large change of $|N_{eff}|$ as measured immediately after irradiation of standard silicon detectors is depicted in figure 8 [8]. The not tolerable increase of the needed depletion voltage after "type inversion" had then been the major impact for radiation hardening.

4.3.1. CERN-scenario measurements

In real applicational scenarios damage induced "immediate" changes of N_{eff} as displayed in figure 8 will always be connected with subsequent "annealing" effects. It was therefore found useful to devise an almost online possibility for rapidly comparing the radiation tolerance between different materials, taking the yearly expected annealing into account. The so called CERN-scenario experiments consist of consecutive irradiation steps with a short

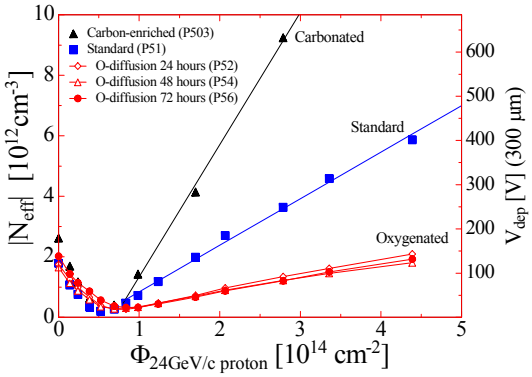

Fig. 9. Influence of carbon and oxygen enrichment to changes of the effective doping concentration after proton irradiation.

term annealing in between [27]. The annealing steps (4 minutes at 80°C) are chosen such that the observed change in N_{eff} corresponds to what would be expected after about 10 days at 20°C. Thus the operational LHC scenario can be approximated this way. The chosen annealing time corresponds also to the minimum of the annealing curve as measured for 80ºC and is therefore closely related to the "stable component" of the change in N_{eff} (see below).

Figure 9 shows a comparison between standard, carbon- and oxygen enriched silicon as irradiated by 23 GeV protons at the CERN PS irradiation facility [27]. It is clearly seen, that the O-enrichment reduces the change in Neff and likewise in the depletion voltage considerably to about 1/3 of that for standard silicon while carbon-enrichment proves to have an adverse effect. However, although pion and proton

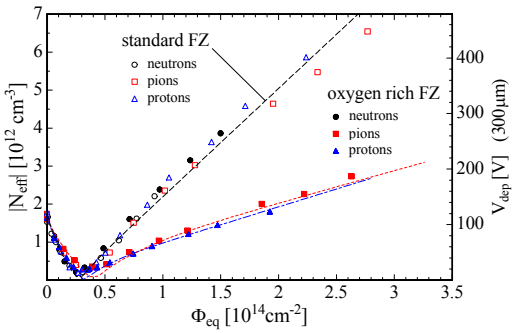

Fig. 10. Particle dependance of radiation damage for standard and oxygenated silicon detectors.

irradiation exhibit the same superiority of DOFZ material, neutron damage does not result in a similar improvement, see figure 10 [27]. This discrepancy with the simple NIEL scaling assumption (section 3) is often been referred to as the "p-n-puzzle". A discussion of this point will be given in section 4.5.1.

4.3.2. Annealing experiments and modeling

As already mentioned, the CERN scenario tests allow only the measurement of one relevant damage parameter, namely the change of the effective doping concentration around the minimum of the annealing function. A different but much more time consuming approach, introduced by the Hamburg group, uses a set of diodes which are irradiated individually with different fluences and are then subjected to full annealing cycles at an elevated temperature for accelerating the annealing kinetics (see [13] and literature cited there). The result of such an annealing experiment is shown in figure 11. ΔN_{eff} is the damage induced change in the effective doping concentration:

$$\Delta N_{eff}(\Phi_{eq}, t(T_a)) = N_{eff,0} - N_{eff}(\Phi_{eq}, t(T_a)) \qquad (3)$$

As function of the equivalent fluence Φ_{eq} and the annealing time t at temperature T ΔN_{eff} can be described as:

$$\Delta N_{eff} = N_A(\Phi_{eq}, t(T_a)) + N_C(\Phi_{eq}) + N_Y(\Phi_{eq}, t(T_a)) \qquad (4)$$

ΔN_{eff} consists of three components, a short term beneficial annealing N_A, a stable damage part N_C and the reverse annealing component N_Y. Both time constants for the beneficial as well as reverse annealing depend strongly on the temperature. A more detailed discussion can be found in [10, 13]. Recent results for the stable damage component N_C have shown that there is no pronounced difference between a moderate 24 h and an enlarged 72 h oxygen diffusion and in fact the improvement with respect to standard material is also only marginal as to be seen in figure 12 [20]. This surprising effect will be further discussed in section 4.6.

A much more general behavior regarding the DOFZ benefits is seen for the reverse annealing amplitude. Standard silicon reveals an almost linear behavior of the reverse annealing amplitude N_Y with fluence while DOFZ silicon shows strong saturation

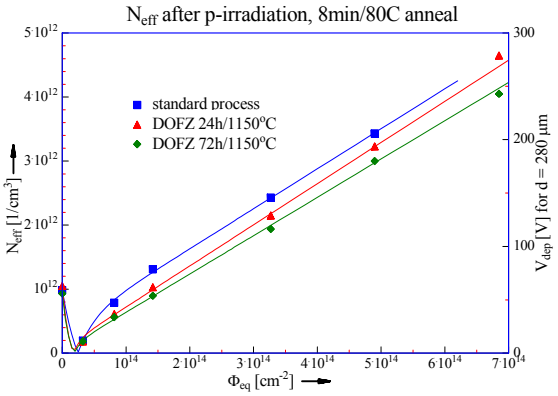

Fig. 12. Stable damage related N_{eff} in minimum of annealing curve after PS-p-irradiation for standard and DOFZ silicon.

at large fluences. This effect as well as an observed increased time constant [1, 20] offer an additional safety margin for detectors kept at room temperatures every year during maintenance periods. As shown in [20] and documented in figure 13, the difference between 24 and 72 h O-diffusion is again not very large. It is however interesting that there are, contrary to previous investigations, also some benefits after neutron irradiation.

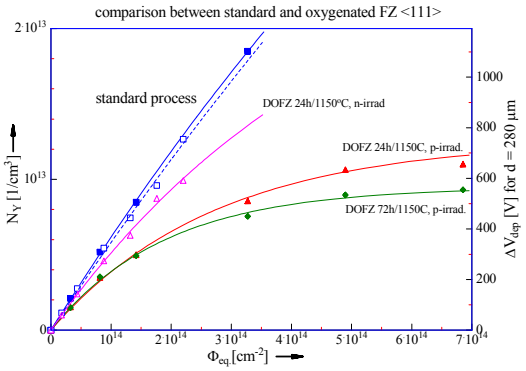

Fig. 13. Reverse annealing amplitude as function of equivalent flunence after n- (open symbols) and PS-p-irradiation (filled symbols). For neutrons the data are normalized to those for protons for the standard process [20].

With all parameters of eq. (4) it is then possible to calculate the expected change of the necessary depletion voltage throughout prolonged operation in any given hadron radiation environment. Such projections on the 10 year LHC operational scenario

are finally shown in figure 14. It is obvious that only the DOFZ method guarantees the required lifetime expectancy of 10 years for the innermost pixel layer of the ATLAS experiment (see also [23]). It should however be emphasized that the damage projection shown here is based on the parameters listed in [1]

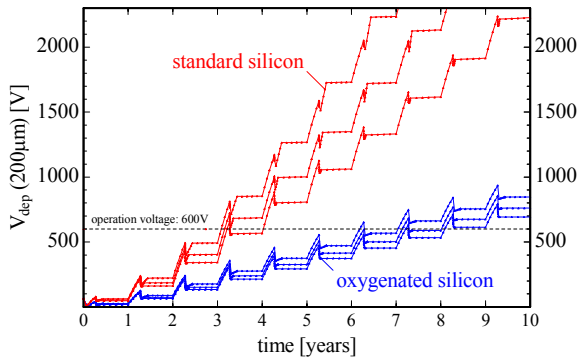

Fig. 14. Damage projections for the ATLAS pixel detector at r = 4cm (B-layer) as an example. Curves from bottom to top: yearly maintenance period at 20ºC: 14, 30 and 60 days [1].

thus may underestimate the beneficial DOFZ effect according to recent results as shown in figure 13 (see also [20]). The actual values seem also to depend on the individual manufacturing process (see section 4.5). It should also be mentioned that annealing experiments have to include a long known bi-stable effect [28]. Thus final conclusions can only be drawn after some proper quality assurance check of the actual detectors.

4.4. Charge collection efficiency

For any application of silicon detectors in vertex detectors the prime focus is on the operating voltage needed to guarantee a sufficiently good S/N ratio for detection of mip's. The signal noise is controlled by operating the detectors at low temperature (–10°C). Such, a good charge collection efficiency is then the prime objective. For best performance full depletion of the detector thickness is needed and therefore the considerations outlined in section 4.3 are of great importance. However, in order to keep trapping and ballistic deficit effects low, the operating voltage has to be even larger than the depletion voltage.

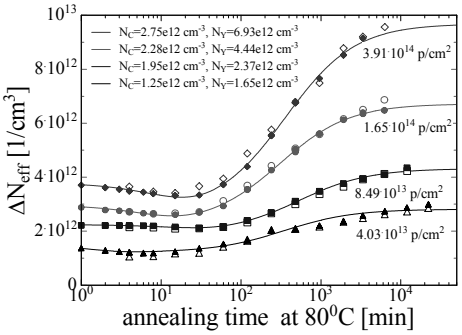

Fig. 15. Annealing curves as measured from charge collection (open symbols) and C/V-measurements (closed ones).

Measurements of charge collection in test diodes have been performed with β-sources and long wavelength infrared laser light pulses, which ensure a near mip like charge track generation throughout the depth of the device (see e.g. [29]). Other experiments have used short wavelength IR laser beams illuminating the test diode from either p^+ or n^+ side for investigation of the electron resp. hole dominated pulse signals separately. This allows the study of charge carrier trapping effects and these results could then again be included in model calculations for LHC or other applications [30-33].

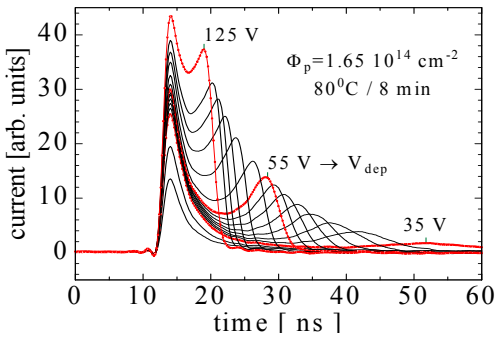

Fig. 16. Time resolved diode signals for 1 nsec IR-laser injection (λ=830 nm) on p^+-electrode, after 1.65·10^{14} p/cm² irradiation [1].

The analysis of charge collection as function of bias voltage should, similar to capacitance/voltage measurements, also reveal the depletion voltage. It is reassuring that in fact both techniques have led to the same results (figure 15) [1]. Examples of time resolved signal pulse shapes are shown in figure 16 [1]. The double peaking is attributed to a double

junction structure of the kind p^+npn^+. This is a generally observed effect and still needs its complete explanation, a likely explanation as also other details of the signal shape are discussed in [34, 35].

The application of charge collection results as obtained with test diodes to segmented detectors is not straight forward but incorporates a more complex calculation involving the geometrical structure of the detector by using a "weighting field". This point had long been neglected and only recently caught more attention, for detailed discussion see [36].

4.5. Microscopic understanding of damage effects

Systematic studies for defect engineering are finally only possible if the correlation between defect formation and the detector performance would be known. Numerous investigations have been undertaken for characterization of damage induced defects in detector grade silicon, especially using DLTS (Deep Level Transient Spectroscopy) and TSC (Thermally Stimulated Current) techniques, showing a lot of relevant results [9, 10, 25, 37-40]. A promising correlation has been reported between the cluster formation as visible in the double vacancy defect and the damage related current [25]. Other studies have given a lot of detailed information of defect kinetics visible in the changes during prolonged annealing or as function of temperature (see e.g. [9, 10, 37]). However despite many partially useful attempts it was so far not possible to quantitatively fully understand the (macroscopic) detector performance on the basis of such (microscopic) data. In the following two examples are given, which are regarded to be promising in this respect.

4.5.1. p-n puzzle, violation of NIEL scaling

As outlined in section 3, originally all damage effects had been assumed to be simply proportional to the displacement damage cross section and hence to obey a universal behavior not depending on the particle type and energy if NIEL scaling is applied. NIEL scaling is still valid for the damage induced bulk generation current of high energy hadron irradiated detectors (section 4.2) but is strongly violated for the change of the effective doping concentration (see section 3, figure 10 and 13).

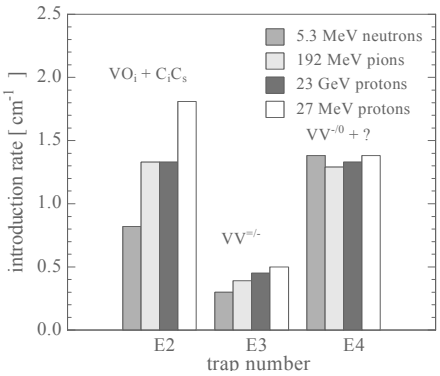

Fig. 17. Generation rates for E2 and E4 as obtained from neutron, pion and proton irradiation (see text): g(E2)/g(E4) = 0.6 (5 MeV neutrons), 1.0 (192 MeV pions and 23 GeV protons) and 1.3 (27 MeV protons).

Although this so called proton-neutron puzzle is still not completely understood, the following remarks may be useful. Figure 17 shows the experimental results of point defect generation rates after n-, p- and pion irradiation [25]. The double vacancy defect E4 is surely related to cluster formation while E2 is composed of the A-center (VO_i) and a carbon complex (C_iC_s), both being discrete point defects. Therefore the ratio of g(E2)/g(E4) measures the point defect generation with respect to cluster formation. These findings may be compared with the simulation results shown in figure 18 [6].

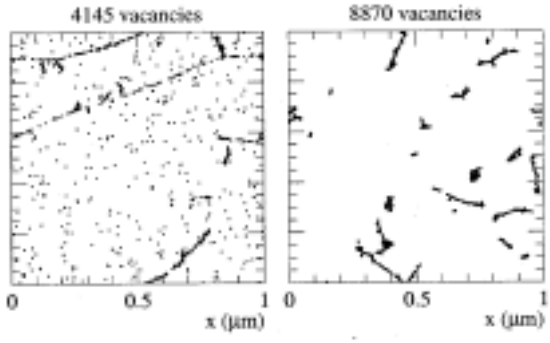

Fig. 18. Initial distribution of vacancies produced by 24GeV/c protons (left) and 1 MeV neutrons (right), corresponding to a fluence of $1 \cdot 10^{14} cm^{-2}$. Simulation result from Huhtinen [6].

1 MeV neutron damage is obviously dominated by the production of cluster like vacancy agglomerates with typical dimensions of 100Å or less while high energy protons lead to an additional concentration of isolated and homogeneously distributed vacancies and interstitials, responsible for point defects. The p-n-puzzle is just a result of the different primary interactions, which are in the case of neutrons caused by hard core nuclear scattering with energy transfers likely larger than the cluster formation threshold of 5 keV. For charged hadrons the Coulomb interaction prevails leading to much lower recoil energies below the cluster threshold thus responsible for more point defects. This clear picture may have to be changed if high energy pion or proton damage would be compared to that produced by neutrons with much larger energies than those accessible in reactors. In fact the neutron energy spectrum in the inner detector of LHC experiments covers a range up to about 100 MeV (figure 3). At this energy secondary nuclear reaction products as e.g. α-particles, protons and even those with larger mass could contribute to low energy recoils due to their Coulomb interaction much more than resulting from 1 MeV neutrons (elastic nuclear scattering only). Thus the p-n-puzzle could indeed be less pronounced if damage studies would be performed with higher energetic neutrons. As a result, if the DOFZ related benefits are closely related to point defect formation as it presently looks (see next section), the actual neutron damage for the tracking detectors might also be reduced by using DOFZ silicon.

4.5.2. microscopic picture of gamma induced damage

Although a lot of microscopic investigations on defect generation induced by hadron irradiation had been performed, it has yet not been possible to relate the macroscopic change in N_{eff} to any such defects in a quantitative way. The long suspected candidate which could explain also the improvement obtained by oxygen enrichment is the acceptor like V_2O-center, a deep defect in the middle of the forbidden gap [41]. In contrast to hadron irradiation low energy gamma damage leads only to the generation of point defects revealing a much cleaner picture not complicated by cluster effects. Co-60 γ-irradiation studies have shown that the improvement obtained

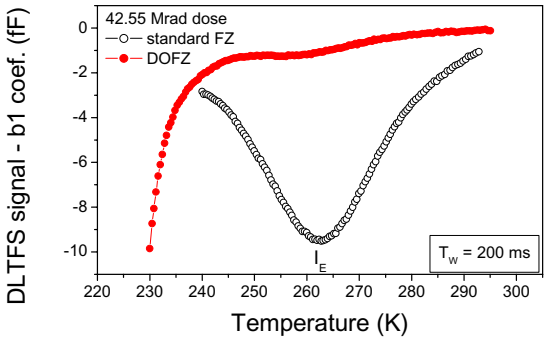

Fig. 19. DLTS spectra showing a close to midgap level at E_a=0.54 eV (V_2O) in standard silicon and suppressed in DOFZ [42, 43].

with DOFZ silicon is in this case much more pronounced than observed after hadron irradiation [42]. Only recently a defect had been measured by DLTS and TSC techniques very likely to be identified as the long searched V_2O center [43, 44]. Its generation is largely suppressed in DOFZ silicon, see figure 19. Effective doping concentration does not show any type inversion as seen in standard material, see figure 20. Using the analyzed defect parameters as function of the gamma dose it was then shown that both the change in the effective doping concentration and reverse current of standard silicon detectors can largely be attributed to the generation of the V_2O center [45]. This result can rightfully be regarded as an absolute first in the long and sometimes frustrating search for an understanding of macroscopic damage effects by defect analysis.

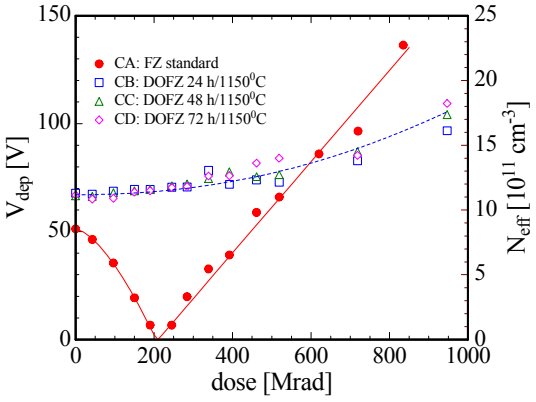

Fig. 20. Effective doping concentration as function of gamma dose for standard (closed) and DOFZ silicon (open symbols) [43].

4.6. Open questions

Although it looks that the final results have led to an almost universal recipe for improving the radiation tolerance in a predictable way and a possibility to perform projections to any operational scenario, a number of problems remain still open.

One of the most asked questions is: how much oxygen is enough? New results suggest that the main positive effect is already achievable with a diffusion for 24 hours at 1150°C ([20], see figures 12 and 13). However such a short diffusion process leads to a pronounced non-homogeneity in the depth profile of the O-concentration (see figure 5), the effect of which is not yet known. A detailed comparison with the BNL HTLT (High Temperature Long Time) DOFZ process resulting in a homogeneous oxygen depth profile would be very interesting [46].

Most test damage experiments have been performed with irradiations of diodes at room temperature and unbiased and hence much different from the actual situation. Only in a few cases the real operational conditions (-10ºC and under bias) had been included. Examples are reported e.g. in [47], [48]. More systematic studies are needed, especially with proton resp. pion irradiation.

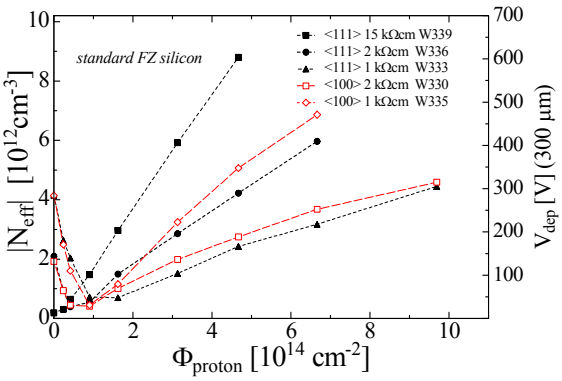

Fig. 21. Stable damage component for DOFZ detectors from different material, manufactured by ST Microelectronics (Italy).

A worrying result of principal importance is illustrated in figures 21 and 22 [49]. CERN scenario experiments with different material have shown that the "stable damage" component as function of fluence varies widely for standard FZ silicon (figure 21), whereas for DOFZ silicon the variations are small (figure 22). The results, shown here only for diodes of one manufacturer, are much more generally

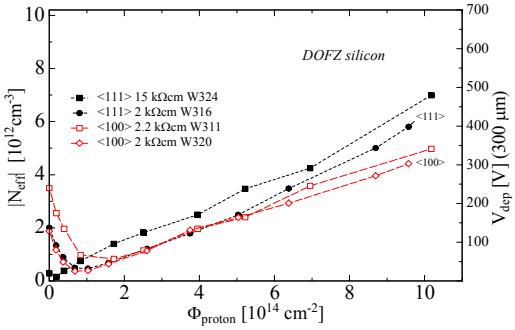

Fig. 22. Same as in Fig. 21 but for various DOFZ silicon.

Valid, including different sources. A likely reason for the effect could be a different carbon content. Reliable material characterization before and after processing will be essential.

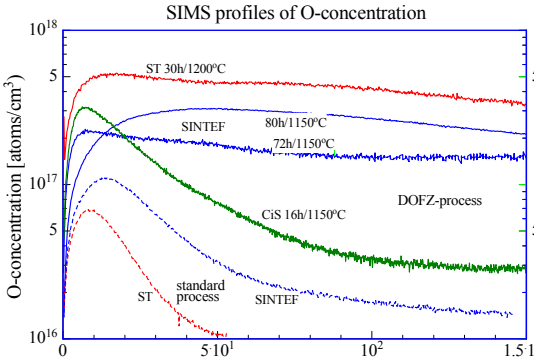

Fig. 23. Depth profiles for oxygen enrichment obtained by different DOFZ processes at various manufacturers: ST: ST Microelectronics (Italy), SINTEF (Norway), CiS (Germany). The bottom 2 curves are for a standard oxidation process, all others diffusion oxygenated as labelled.

Another riddle is displayed in figures 23 and 24 [50]. Here the correlation between the oxygen enrichment and its results for the saturation of the reverse annealing is demonstrated. In general one observes the expected effect: a larger O-concentration leads to lower reverse annealing amplitudes. E.g. the standard ST Microelectronics process (bottom most curve in figure 23) reveals the lowest O-concentration and shows the largest N_Y values (top

curve in figure 24). Also the ST-process with the largest O-concentration (30h at 1200°C, top curve in figure 23) results in the best reverse annealing performance (bottom most curve in figure 24). Although the CiS process (16h at 1150°C, 3rd curve from bottom in figure 23) and the SINTEF process (72 resp. 80h at 1150°C, 4th and 5th from bottom in figure 23) show the expected difference in the O-concentration , the reverse annealing obtained with the CiS diodes (2nd from bottom in figure 24) is better than that for the SINTEF process (3rd and 4th from bottom in figure 24). This quite confusing result may be understood by differences induced from the individual process. Characterization of the material after processing is therefore urgently needed, an example is given in [51].

5. Recent studies for improvements

The normal oxygen enrichment via the DOFZ process makes use of the diffusion of oxygen present as single atoms on interstial lattice sites. A modification had been introduced by the Brunel group generating oxygen dimers (2 closely related interstitial O-atoms). First damage studies with such material have shown promising results with evidence for the reduction of cluster related damage [52].

The BNL group, using their HTLT technique have additionally doped the material with thermal donors. An appreciable improvement had been reported showing no increase of the stable damage component of N_{eff} at proton fluences above $2 \cdot 10^{14}$ p/cm² [46].

Finally the Hamburg group had performed damage tests with diodes fabricated from high resistivity Czochralski silicon, which has an as grown O-concentration of $8 \cdot 10^{17}$/cm³ (see also figure 5), much larger than possible with any DOFZ process. First damage experiments with pion and proton irradiation have shown no type inversion after large fluences, an effect which is in contrast to all FZ results and could indeed be very profitable for detector applications [20].

6. Conclusions

- Diffusion oxygenation of float zone silicon (DOFZ) has proven to be a powerful technique for reducing damage effects in silicon. Model parameterization of damage effects allows the calculation of detector performance for long term LHC operation.
- The DOFZ method had been successfully transferred to several detector manufacturers. It will be used for part of LHC strip and pixel detectors.
- There are still a number of open questions regarding the ROSE results. Among them are: Optimization of the O-enrichment, a possible dependence of damage effects on the initial silicon material and on the individual process technology.
- Recent updates of ROSE results have shown that the DOFZ process reveals also benefits for neutron irradiation. It is argued that these will even be larger if tests would extended to higher neutron energies, relevant for the LHC tracking area.
- An absolute first in understanding the diode performance on a microscopic level is reported for Co-60 gamma irradiated silicon.
- New studies have shown further improvements for the radiation tolerance of silicon by oxygen dimerization, dedicated doping with thermal donors and by replacing float zone with Czochralski grown silicon.
- Finally it should be mentioned that a new international collaboration had been initiated and approved by CERN as RD50, which will focus on the development of radiation hard semiconductor devices for very high luminosity colliders [53].

Acknowledgements

The author wishes to express his thanks to the whole ROSE community for their numerous contributions, which have been reviewed in this report. I am very grateful to M. Moll (CERN) for many comments and help in collecting the presented

material. The most recent results have been obtained in collaboration with CiS (Erfurt, Germany) under contract CiS-SRD 642/06/00. Finally many thanks are especially due to E. Fretwurst, I. Pintilie, J. Stahl and the whole Hamburg group for many invaluable discussions and untiring technical assistance.

References

[1] RD48 Status report, CERN/LHCC 2000-009, December 1999; G. Lindström et al.(ROSE), Nucl. Instr. and Meth. A 466 (2001) 308; The ROSE Collaboration in: http://rd48.web.cern.ch/RD48
[2] CERN-RD39 in: http://rd39.web.cern.ch/RD39
[3] S. Parker et al.; Performance of 3D architectured silicon sensors after severe proton irradiation, to be publ. in IEEE TNS and refernces cited there.
[4] ROSE publications, status reports, technical reports and workshops, in: http://rd48.web.cern.ch/RD48
[5] J. Wüstenfeld, Ph.D. thesis, Dortmund 2001, Internal Report UniDo PH-E4 01-06, August 2001, see also ROSE/TN/2000-05 in [4]
[6] M. Huhtinen, Simulation of non-ionizing energy loss and defect formation in silicon, Nucl. Instr. And Meth. A, to be publ., see also ROSE/TN/2001-02 in [4]
[7] S.J. Watts in: 5th ROSE workshop (2000) 452, CERN/LEB 2000-005; Radiation Effects in Silicon Detectors, 1st ENDEASD workshop April 21-22 (1999) 93
[8] R. Wunstorf, Ph.D. Thesis, University of Hamburg 1992, DESY FH1K-92-01, 1992
[9] H. Feick, Ph.D. thesis, University of Hamburg 1997, DESY F35D-97-08, 1997
[10] M. Moll, Ph.D. thesis, Hamburg University, 1999, DESY-THESIS-1999-040, ISSN-1435-8085
[11] ASTM E722-85, ASTM E722-93 (revised)1993
[12] A. Vasilescu and G. Lindström, ROSE TN/2000-02 in [4]
[13] G. Lindström et al., Nucl. Instr. and Meth. A 426 (1999) 1
[14] P.J. Griffin et al., SAND92-0094 (Sandia Natl. Lab. 93) and private communication
[15] A. Konobeyev, J. Nucl. Mater. 186 (1992) 117
[16] M. Huhtinen and P.A. Aarnio, Nucl. Instr. and Meth. A335 (1993) 580 and HU-SEFT-R-1993-02 (1993)
[17] G.P. Summers et al., IEEE NS40 (1993) 1372
[18] A. Akkerman et al., Radiat. Phys. Chem. 62 (2001) 301
[19] Z.Li and H.W. Kraner, BNL-46198, J. Electron. Mater. 21 (7) (1992) 701
[20] E. Fretwurst et al., Developments for radiation hard silicon detectors; 4th International Conference Radiation Effects on Semiconductor Materials, Detectors and Devices, July 10-12, Florence, Italy, to be publ. In Nucl. Instr. and Meth. A
[21] A. Barcz et al., Extremely deep SIMS profiling : Oxygen in silicon, SIMS XIII conference, Nov. 2001, Nara (Japan), to be publ. in Applied Surface Science
[22] SINTEF (Norway), CiS (Germany), STMicroelectronics (Italy), IMB-CNM (Spain); see also: L. Fonseca et al., Microelectronics Reliability Vol 40 (4-5) (2000) 791
[23] R. Wunstorf, Nucl. Instr. and Meth. A 466 (2001) 327
[24] M. Moll et al., Nucl. Instr. and Meth. A 426 (1999) 87
[25] M. Moll et al., Nucl. Instr. and Meth. B 186 (2002) 100
[26] B. C. MacEvoy et al., Physica B: Condensed Matter 273 (1999) 1045; F. Moscatelli et al., Nucl. Instr. and Meth. B 186 (2002) 171
[27] A. Ruzin et al., Nucl. Instr. and Meth. A 447 (2000) 116
[28] M. Moll et al., Nucl. Phys. B 44 (Proc. Suppl.) (1995) 468
[29] G .L. Casse et al., Nucl. Instr. and Meth. A 426 (1999) 140
[30] G. L. Casse et al., Nucl. Instr. and Meth. A 466 (2001) 335
[31] E. Fretwurst et al., Nucl. Instr. and Meth. A 388 (1997) 356
[32] T.J. Brodbeck et al., Nucl. Instr. and Meth. A 455 (2000) 645
[33] G. Kramberger et al., Nucl. Instr. and Meth. A 476 (2002) 645
[34] V. Eremin et al., Nucl. Instr. and Meth. A 476 (2002) 537
[35] E. Verbitskaja, 6th ROSE workshop October 2000, CERN/LEB 2000-06 (2000) 363
[36] G. Kramberger, Ph.D. thesis University of Ljubljana 2001 and IEEE-TNS 49 (4) August 2002, to be published
[37] M. Moll et al., Nucl. Instr. and Meth. A 388 (1997) 335
[38] I. Pintilie et al., APL 78 (2001) 550
[39] M. Kuhnke et al., Nucl. Instr. and Meth. B 186 (2002) 144
[40] Z. Li et al., Nucl. Instr. and Meth. A 476 (2002) 628
[41] B. C. MacEvoy, Nucl. Instr. and Meth. A 388 (1997) 365
[42] Z. Li et al., Nucl. Instr. and Meth. A 461 (2001) 126
[43] I. Pintilie et al., Appl. Phys. Lett. 81, No 1 (2002) 165
[44] I. Pintilie et al., Preliminary results on defects induced by Co-60 gamma irradiation in oxygenated and standard silicon, conference contribution presented at the 4th International Conference on Radiation Effects on Semiconductor Materials, Detectors and Devices, July 10-12, Florence, Italy, to be publ. in Nucl. Instr. and Meth. A
[45] E. Fretwurst et al., Bulk damage in standard and oxygen enriched silicon detectors induced by Co-60 gamma irradiation, conference contribution presented at the 4th International Conference on Radiation Effects on Semiconductor Materials, Detectors and Devices, July 10-12, Florence, Italy, to be publ. in Nucl. Instr. and Meth. A
[46] Z. Li et al., Nucl. Instr. and Meth. A 461 (2001) 126
[47] F. Anghinolfi et al. (RD2 collaboration), Nucl. Instr. and Meth. A 326 (1993) 365
[48] V. Cindro et al., Nucl. Instr. and Meth. A 476 (2002) 565
[49] M. Moll, private communication, data compiled from ROSE results, see M. Moll, CERN Detector Seminar, 14-Sep-01
[50] G. Lindström et al., Nucl. Instr. and Meth. A 465 (2001) 60
[51] J. Stahl et al., Deep defect levels in standard and oxygen enriched silicon before and after gamma irradiation, this conference
[52] C. daVia and S. J. Watts, Nucl. Instr. and Meth. B 186 (2002) 111
[53] R&D proposal: Development of radiation hard semiconductor devices for very high luminosity colliders, CERN report, LHCC 2002-003/P6 (Feb. 2002) http://www.cern.ch/rd50/